BIOMECHANICS OF A SINGLE LAP IN VITRO MODEL FOR INTEGRATED ARTICULAR CARTILAGE

J. Fierlbeck*, J. Hammer*, C. Englert** and R.L. Reuben***

*Labor für Werkstofftechnik und Metallographie, University of Applied Sciences Regensburg, Regensburg, Germany
**Hospital of University of Regensburg, Department of Trauma Surgery, Regensburg, Germany
*** Heriot-Watt University, School of Engineering and Physical Sciences, Edinburgh, UK,

jfierlbeck@lwm-regensburg.de

Abstract: A variety of orthopaedic pathologies and treatments result in mechanical defects of the articular cartilage. Successful therapeutic interventions require either direct repair of the native tissue or, in the case of serious trauma, partial replacement of the cartilage defect by appropriate tissues. In the later case, the post operative outcome is inseparably related to integration, cell vitality and load bearing capacity of the biomaterial. Most of the *in-vitro* models for articular cartilage integration describe these properties by mechanical, biochemical and histological analysis, respectively. Generally, the quality of the adhesive joint can be investigated by the resulting mechanical properties of the tissue.

The aim of this study is to analyse the mechanical strain distribution in a single lap configuration by means of an optical strain measurement system. Supportive finite element computation is performed to indicate the heterogeneous strain distribution in the integration area, concerning geometrical effects of the single lap model.

These results lead to a better interpretation of the mechanical behaviour of articular cartilage integration in *in-vitro* models using a single lap configuration.

Introduction

In joint trauma or disuse articular cartilage defects are the first step in the development of osteoarthritis [1, 2]. To prevent osteoarthritis in such cases therapeutic interventions are required in order to achieve direct repair of the native tissue or partial replacement [1-6] of the load bearing capacity of the interface with native-to-native or native-to-tissue-engineered cartilage [7, 8]. In order to achieve complete repair of the joint, it is important that the repaired and surrounding tissue shows homogeneous elastic behaviour at least to the extent of the original cartilage. The mechanical properties of the tissue are related to cell vitality, biochemical composition and structure [5] and therefore, to the quality of articular cartilage integration [9, 10]. *In vitro* analysis of the articular cartilage integration process has identified the key role of collagen metabolism and structure in determining the mechanical properties of the interface. Cross linking [10-12] and the extent of alignment of the molecules, and hence the structure and morphology of the collagen fibres, influence the mechanical integrity in much the same way as they do in synthetic polymers. Most published mechanical *in vitro* analysis of integration lacks the comparison with native tissue [13], although, native integrity characteristics are of importance to establish if an adhesive tissue has resulted from the integration. Accordingly, this work focuses on the strain characteristics of native to native articular cartilage tissue, cultured in a single lap configuration for 14 days [11].

However with such a simple specimen configuration and monotonic tensile loading (Figure. 1a), the strain distribution in the sample is quite complex. The set-up offers loading conditions similar to those *in vivo* where articular cartilage surfaces oppose each other or in trauma or under surgical interventions [4, 5]. High resolution measurement of local strain distributions in the integration area allows a specific focus on the mechanical properties of the new repair tissue and the influences of the used model. Generally, the results are analysed in terms of the adhesive strength and total strain at rupture, as this ultimately matters in the clinical situation. Whereas, the transition from native to repair tissue of every sample induces strain dependent inhomogeneous deformation of the integration specimen [14], the apparent adhesive strength and the gradients in local strains can be regarded as practical parameters, providing useful information concerning the individual quality of the integrated tissue [10].

Materials and Methods

One knee joint of a 6 week-old calve was provided by a local slaughterhouse 4 hours after death. Full-thickness osteochondoral cubes (12 mm x 10 mm) were harvested from the patellafemoral groove. Slices parallel to the superficial zone, 250 μm in thickness were cut by a microtome (Microm HM 440E), and the first two slices discarded to dispose of the top layer of curved articular surface. The next slice of 250 μm thickness was preserved in a 24-well culture plate. Geometrically defined cartilage specimens (8 mm × 2.5 mm × 250 μm) were punched out of the slices in two steps using two specially designed blade scalpels.

ISSN: 1727-1983

During all preparation steps the specimens were kept moist with PBS or stored at 4 C° in PBS.

For incubation, two strips were positioned one above the other with an overlapping area of 4 mm × 2.5 mm (10 mm^2), (Figure 1a), which results in a total length of 12 mm for all specimens after integration.

The integrative property was influenced by ascorbate with standard medium in drug dose response manner. These data showed in a preliminary investigation optimum stimulation of biomechanical integration with a concentration of 100µg/ml of ascorbate. Ten specimens were used for this mechanical investigation.

The adhesive strength of the repaired tissue was measured under tensile loading using a specially modified tensile testing machine (Hegewald & Peschke). Two spring loaded clamps with a defined gripping force, adjustable between 0 and 20 N, provided sufficient grip and fixation stability to minimize effects on the registered displacement data and avoid slipping of the specimen. The gauge lengths of the samples were 7 mm in all experiments. A tensile preload of 0.05 N was applied prior to testing. Samples were deformed until rupture at a nominal speed of 1 mm/min. Displacement and load was recorded by an internal linear variable displacement transformer (LVDT) of the test rig and a 100 N load cell (Hottinger Baldwin). The accuracy of the nominal deformation and load signals were $\pm 1 \times 10^{-3}$ mm and ±0.01 N, respectively. In parallel with these integral measurements an optical deformation measurement system (ARAMIS, GOM) was used to investigate the local deformations and strains. Specific emphasis was put on the integration area (region A) and the cartilage strips connected to the gripping (region B) (Figure 1b), to evaluate the influence of this sections concerning the total integral deformation. The strain of region A is calculated by the individual length of the integration area and the elongation in tensile direction. The length of region B is determined by the deviation of the gauge length of 7 mm and the specific length of the integration area of each sample. The displacement is measured by the optical system. The integral strain is calculated by the ratio of displacement at rupture to initial gauge length using the internal LVDT.

Nonlinear finite element analysis was used to model geometrical effects in more detail and to provide information about the stress - strain distribution in the integration area. The native tissue properties were modelled with a linear elastic material law (Young`s modulus of 25 MPa and a Poisson's ratio of 0.3) [15]. The newly grown tissue was modelled by using a bilinear isotropic material law with a Young`s modulus of 5 MPa, a Poisson's ratio of 0.3, a yield stress of 0.07 MPa, and a post yield slope of 0.75 MPa, respectively. These parameters are assumptions from results of single lap tests with integral deformation measurement. The thickness of the integration area was taken to be 30 µm which is the average determined from histological analysis of the cross sections. It should be noted that crack propagation and element failure were not considered in the model. All computations were performed with the finite element code ANSYS 8.1.

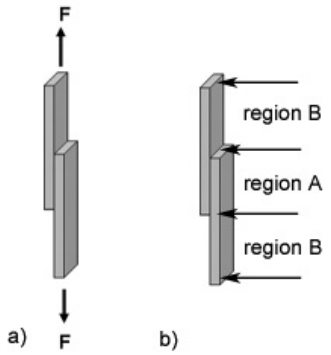

Figure 1: Geometry and load case of the single lap specimen (a); regions of detailed strain analyse (b).

Results

The integral deformation behaviour of the integrated bovine articular cartilage specimens is characterized by the typical performance of articular cartilage under tensile load. The force displacement diagram shows the nonlinear "toe" region (minimized due to the applied preload), followed by a linear part until rupture of the integration area occurs [15] (Figure 2). The point in the diagram indicates the average value and standard deviation of all samples concerning force und elongation at rupture. This force normalised to the individual integration area of the specimen results in an average failure stress of 67 kPa ± 15 kPa. Concering the average displacement at rupture, region A shows 53 % and region B 47 % of the total elongation.

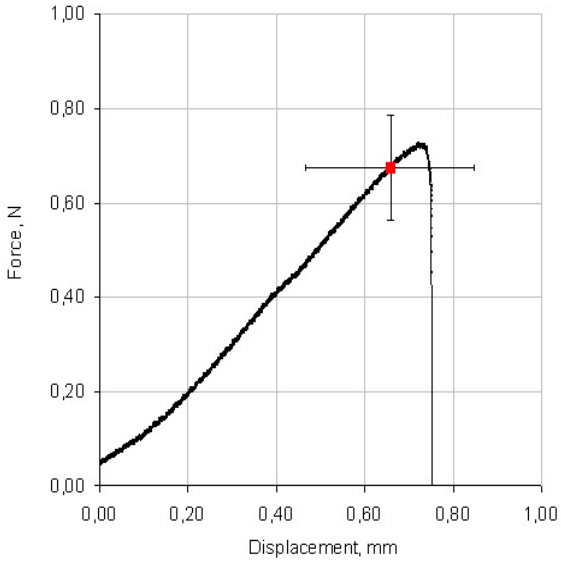

Figure 2: Typical load displacement result curve and maximum displacement at failure versus load of all specimens (n=10).

Figure 3 shows the partial strain distribution measured on the specimen surface in region A, B and the total strain at rupture. The integration area exhibits average strains of 8.2 ± 2.7 % where the end pieces

ISSN: 1727-1983

(region B)of the specimens show strain values of 11.5 ± 3.8 %. The total strain determined is 9.2 ± 2.6 %.

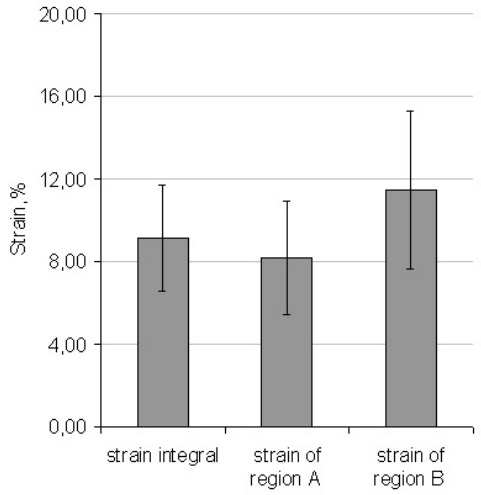

Figure 3: Average values of integral and partial strains of the single lap configuration (region B includes upper and lower section), black bars indicate standard deviation (n = 10).

Additionally to these partial investigations a typical local strain pattern is represented by Figure 4. The image shows the highly heterogeneous strain distributions in a front view of the specimen. The strains are concentrated in the upper and lower extremities of the integration area (where the thickness changes from double to the initial cartilage thickness). In this transition the local strains are up to 20 % higher comparable to those on the free surfaces of the laps. Also typical for the samples are the curved areas showing identical strain levels, indicating decreasing values to the centre of the integration area. The region marked with a circle exhibits best integration performance.

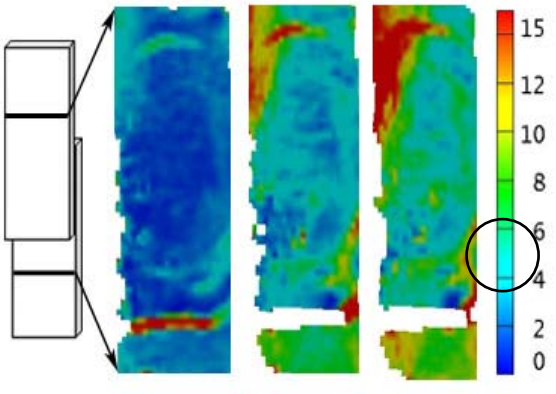

Figure 4: Von Mises strain distribution in % on the specimen front view of the integration area; location and strain levels for loads of 0.25, 0.66, and 0.78 N (from left to right).

The finite element computation was focused on assessing how the geometry affects the strain distribution along the gauge section of the specimen and the integration area. Figure 5a shows the calculated strains along the free length of the specimen for a load of 0.9 N. Clearly, the peak strains are at the margins of the integration area, with a high strain gradient, continuously increasing from the centre to the upper and lower margins of the synthesised tissue. The calculated strains are somewhat less than the experimental strain data, suggesting that the chosen values of yield stress or Young's modulus (or both) are too high. Detailed calculations of the stress distribution at loads of 0.3 0.6 (not shown) and 0.9 N reveal a highly heterogeneous stress distribution in the integration area, (Figure 5). With increasing load the equal strain states form the periphery of ellipses with coincident centres.

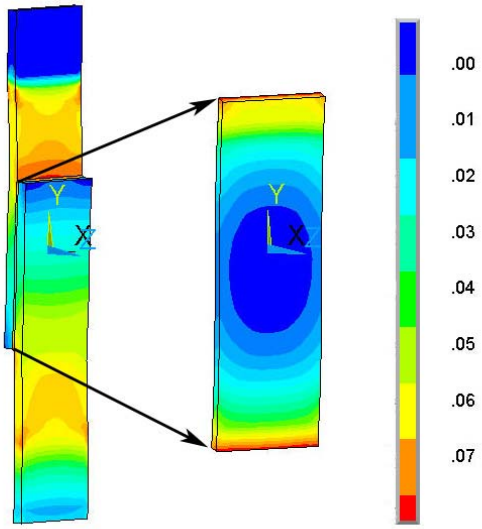

Figure 5: Von Mises strain distribution (mm/mm) over the whole specimen at a peak load of 0.9 N and in detail within the integration area for equal load.

Discussion

The single lap integration model is very useful for the analysis of how mechanical stability is affected by modifications during incubation, where different cultivation media result in different rupture stresses [9, 10, 12, 13]. The description of the mechanical properties of the new synthesised tissue directly is rather complex especially using this model. The failure stresses normalized to the integration area are considered to be an appropriate estimation of the load bearing capacity of the new synthesized tissue. But, the inhomogeneous strain and also stress situation resulting from the geometry of the single lap model, as well as the fact that biological integration does not take place homogenously, it is expected that the real locally acting failure stresses will be higher. The global analysis of the experiment using the crosshead displacement data shows almost linear behaviour, although, this linearity, especially before rupture, it is assumed to be an accumulation of different nonlinear mechanisms. One reason for this integral linearity may be the comparable strain behaviour of the specimen ends under tensile

ISSN: 1727-1983

loading and the complex mixture of interactions in the integration area. Both scopes exhibit about 50 % of the total elongation. This fact is a limiting factor concerning this model and its useful application for integration experiments with high expected rupture stresses. The requirement for a stiff material and a, in comparison, weak adhesive is no longer achieved [16].

The advantage of this model compared to in vitro defect repair models [17] working with pullout tests, is the zero stress condition of the single lap specimen before mechanical testing. All forces measured in this model are directly related to the adhesive bond without any influences of friction.

One important aspect of models concerning the repair quality of soft tissue should be a constant and homogeneous load case during the hole experiment.

Conclusions

The capabilities of a single-lap test for assessing articular cartilage integration have been examined using samples at early stages of integration.

It has been found that a simple load-displacement trace is suitable for measuring the integration quality, provided that the adhesive strength does not approach that of the native cartilage. To investigate cartilage repair tissue comparable to native tissue other models will have to be applied.

References

[1] BUCKWALTER, J. A. (1995): 'Osteoarthritis and articular cartilage use, disuse, and abuse: experimental studies', J Rheumatol Suppl, **43,** p. 13-5

[2] BUCKWALTER, J. A. AND HUNZIKER, E. B. (1996): 'Orthopaedics. Healing of bones, cartilages, tendons, and ligaments: a new era', Lancet, **348 Suppl 2,** p. sII18

[3] BUCKWALTER, J. A. (1983):'Articular cartilage', Instr Course Lect, **32,** p. 349-70

[4] BUCKWALTER, J. A. AND MANKIN, H. J. (1998): 'Articular cartilage repair and transplantation', Arthritis Rheum, **41,** p. 1331-42

[5] BUCKWALTER, J. A. AND MANKIN, H. J. (1998): 'Articular cartilage: degeneration and osteoarthritis, repair, regeneration, and transplantation', Instr Course Lect, **47,** p. 487-504

[6] BUCKWALTER, J. A. AND MANKIN, H. J. (1998): 'Articular cartilage: tissue design and chondrocyte-matrix interactions', Instr Course Lect, **47,** p. 477-86

[7] OBRADOVIC, B., MARTIN, I., PADERA, R. F., TREPPO, S., FREED, L. E. AND VUNJAK-NOVAKOVIC, G. (2001): 'Integration of engineered cartilage', J Orthop Res, **19,** p. 1089-97

[8] HUNZIKER, E. B. AND ROSENBERG, L. C. (1996): 'Repair of partial-thickness defects in articular cartilage: cell recruitment from the synovial membrane', J Bone Joint Surg Am, **78,** p. 721-33

[9] DIMICCO, M. A. AND SAH, R. L. (2001): 'Integrative cartilage repair: adhesive strength is correlated with collagen deposition', *J* Orthop Res, **19,** p. 1105-12

[10] DIMICCO, M. A., WATERS, S. N., AKESON, W. H. AND SAH, R. L. (2002): 'Integrative articular cartilage repair: dependence on developmental stage and collagen metabolism', Osteoarthritis Cartilage, **10,** p. 218-25

[11] AHSAN, T., LOTTMAN, L. M., HARWOOD, F., AMIEL, D. AND SAH, R. L. (1999): 'Integrative cartilage repair: inhibition by beta-aminopropionitrile', J Orthop Res, **17,** p. 850-7

[12] REINDEL, E. S., AYROSO, A. M., CHEN, A. C., CHUN, D. M., SCHINAGL, R. M. AND SAH, R. L. (1995): 'Integrative repair of articular cartilage in vitro: adhesive strength of the interface region', *J* Orthop Res, **13,** p. 751-60

[13] ENGLERT, C., MCGOWAN, K. B., KLEIN, T. J., GIUREA, A., SCHUMACHER, B. L. AND SAH, R. L. (2005): 'Inhibition of integrative cartilage repair by proteoglycan 4 in synovial fluid', Arthritis Rheum, **52,** p. 1091-9

[14] AHSAN, T. AND SAH, R. L. (1999): 'Biomechanics of integrative cartilage repair', Osteoarthritis Cartilage, **7,** p. 29-40

[15] MOW, V. C., GU, W. Y. AND CHEN, F. H. (2005): 'Structure and Function of Articular Cartilage and Meniscus', Lippincott Williams & Wilkins, Philadelphia, p.

[16] ASTM (1992): 'Standard test method for measuring strength and shear modulus of nonrigid adhesives by the thick- adherend tensile lap specimen', American Technical Publishers, Philadelphia, p.

[17] HUNTER, C. J. AND LEVENSTON, M. E. (2004): 'Maturation and integration of tissue-engineered cartilages within an in vitro defect repair model', Tissue Eng, **10,** p. 736-46

ISSN: 1727-1983